



Reflection and damping of linear water waves by a multi-porosity vertical porous structure placed on a step-type raised seabed

Subhadra Mishra¹ · Sunanda Saha² · Santu Das³ · Swaroop Nandan Bora⁴

Received: 17 February 2021 / Accepted: 13 June 2021 / Published online: 8 July 2021
© Sociedade Brasileira de Engenharia Naval 2021

Abstract

With the consideration of linear water wave theory, the problem of water wave reflection by a breakwater in the form of a vertically positioned finite porous structure is studied. The porous structure is placed on a raised impermeable seabed with p -steps and with support from a solid wall at one end. The porous structure contains a number of vertical strips with distinct strip-wise porosity. An oblique wave is assumed to propagate through this specific structure and it gets reflected by the step-like seabed and the vertical solid wall simultaneously. Accordingly, a number of boundary value problems corresponding to region-wise velocity potentials are established for the unbounded water region and the vertical strips of the porous structure. Utilization of the matching conditions along the vertical boundaries between two consecutive designated regions (including the water region) leads to a system of linear algebraic equations which is solved to obtain the reflection coefficient. Further, the study of the reflection coefficient with respect to several distinct parameters is carried out with a focus on the cases for which the coefficients of the wave reflection have low values. The effect of various admissible parameters, namely the wavenumber, the number of steps on the seabed, the number of evanescent modes, the structural width, and the angle of incidence, on reflection coefficient is studied which clearly establishes a significant influence of such parameters on wave reflection. It is observed that, up to a critical value, lower values of reflection coefficient correspond to higher values of angle of incidence. It is also observed that the reflection coefficient reduces corresponding to increasing values of the wavenumber. Therefore, if we consider waves of greater wavelength, then it results in smaller reflection coefficient. The multi-sliced porous structure gives a wider range of angles of incidence where the reflection coefficient keeps decreasing compared to the uniform structure porosity and this configuration is more advantageous for using such a structure acting as a breakwater. Another engineering aspect of the current formulation is the possibility of shuffling of porosity values in the blocks. An optimized porous structure can be engineered with the help of the porosity shuffling. The effectiveness of the present model is justified through a comparison with the available results in the literature.

Keywords Multi-porosity structure · Oblique wave · Reflection · Matching conditions · Multi-step seabed

List of Symbols

ρ Density of water
 ω Angular frequency of the incident wave

f_j Linearized friction factor of the j th region
 S_j Inertial coefficient in the j th region
 d Grain size of the porous material of the structure
 ν Kinematic viscosity
 \tilde{R}_j Dimensionless impedance of each porous region
 p Number of porous strips
 $\Phi_w(x, y, z, t)$ Complex velocity potential in the water region
 g Acceleration due to gravity
 $\Phi_j(x, y, z, t)$ Complex velocity potential in the porous region
 i Imaginary quantity = $\sqrt{-1}$
 γ_j Porosity of j th region of the porous structure

✉ Swaroop Nandan Bora
swaroop@iitg.ac.in

¹ StudyMode Technologies Pvt. Ltd., Koramangala, Bengaluru 560034, India

² School of Advanced Sciences, Vellore Institute of Technology, Vellore 632014, India

³ Mathematical and Computational Sciences Division, Institute of Advanced Study in Science and Technology, Paschim Boragaon, Guwahati 781035, India

⁴ Department of Mathematics, Indian Institute of Technology Guwahati, Guwahati 781039, India

C_M	Added mass coefficient
h_1	Height of the water region
L	Width of the porous structure
h_{j+1}	Height of the j th porous region
λ	Wavenumber in the y -direction
θ	Angle of incidence to the x -axis
$k_{w,0}$	Incident wavenumber
$K_{j,n}$	Wavenumber in the x -direction
R_n	Complex reflection coefficient
N	Number of evanescent wave modes

1 Introduction

Numerous coastal zones worldwide have been known to be disintegrated by water waves, and such threats may thus be present in most of the coastal regions. Some preventive action or installing protective structures is required in these regions either to diminish the hazards or to forestall them from happening. Thus, the study of designing and construction of various types of breakwaters has received a reasonable importance owing to their enormous influence on a number of activities in oceans. An increasing number of activities in the coastal regions have been observed due to the compulsion on the part of some countries in their effort in building several coastal facilities and in finding means to protect these. Furthermore, an upward trend in global trading has resulted in large expansion in harbor traffic which is largely responsible in deteriorating the prevailing conditions around it. For further information in this context, one may refer to Chanda and Bora [3].

The reflection and damping of waves by porous structures is considered to be a very important aspect for the study of designing breakwaters. To avoid a high wave reflection, a porous structure is considered more appropriate than a solid structure. Thus, porous structures are seen to be widely used as breakwaters in coastal regions in providing safety to harbors, ports, inlets, beaches, etc., from unpredictable and harsh wave actions. Further, these structures also act as dissipating seawalls for achieving wave energy attenuation. From engineering perspective, breakwaters usually consist of composite materials or layered armor of material having different values of porosity. Furthermore, porous structures are quite amicably utilized in laboratories as absorbers in experiments to discard unwanted waves. Some other naturally formed porous structures include the likes of muddy or sandy seabed through which water can penetrate through the seabed, and the underwater vegetation field which resists the wave motion and dissipate incoming wave energy. In order to understand the underlying physical processes properly, it is necessary to formulate the boundary value problem correctly since many parameters are involved for a flow through any porous medium. Many researchers starting from nineteenth

century have been actively working in this area to understand the model comprising of porous structure(s). Some of the important works related to the above study are discussed below.

Sollitt and Cross [28] can be considered as pioneers in introducing an effective model which accounted for a wave-induced flow in a porous medium and till date, it has found its place as one of the most widely used model. This approach took into account the dissipative wave energy within a porous medium by invoking a linearized friction term that could be computed by following a procedure with iterative steps as given in Madsen [17] (see “Appendix 1” for more details). Following a similar approach, Madsen [16] evaluated reflection and transmission coefficients due to the normal incidence of long waves interacting with a rectangular porous structure by considering linear governing equations and flow resistance formula. Madsen [17] studied various aspects of the reflection of linear shallow water waves by a bottom-mounted vertical porous structure. These significant works are the stepping stones of the related area of study based on which various researchers at subsequent times included different parameters in the formulation to study more complex problems. Some of those important extensions are mentioned below.

Losada et al. [15] carried out an extension of the investigation conducted by Madsen [17] to discuss the reflection of an oblique incident wave by a homogeneous and vertical porous structure of infinite length. By considering a realistic seabed of varying depth and a porous seawall, Mallayachari and Sundar [18] analyzed various aspects of wave reflection with respect to parameters such as the porosity and friction of the wall, and the relative wall width. This experiment showed that the reflection coefficient reduced with an increase in the porosity and with an increase in the wall width. Chamberlain and Porter [2] and also Porter and Staziker [21] employed the variational principle and Galerkin method in studying water wave refraction and diffraction by an undulating seabed and obtained an equation similar to the one obtained by Mallayachari and Sundar [18]. Further, Zhu [37] applied wave-induced refraction–diffraction equations for propagation of waves through a porous structure of a reasonable size for which the orthogonal property of the Galerkin eigenfunctions was appropriately used. Das and Bora [5, 6] considered an extension of the work by Zhu [37] to study the reflection of oblique water waves by a finite vertical porous structure placed on an elevated horizontal impermeable seabed and also on a multi-step impermeable seabed. In a further extension by Das and Bora [4], a vertical porous structure at two locations—near and away from the wall—was considered and the associated wave damping was investigated.

It is obvious that breakwaters used in oceans have different geometries such as porous cylinders and thin vertical

barriers. Significant development has taken place in this direction and it is deemed pertinent to discuss a few important works involving such studies. Yu [36] derived a result for water wave propagation through a breakwater in the form of a thin porous structure in a sea of finite depth. It was found that, in the event of neglecting the inertial effect of the structure, the performance of the structure turned out to be an underestimate. Williams and Li [34] studied the interaction of water waves with a cylindrical breakwater system consisting of a semi-porous cylinder and a rigid vertical circular cylinder placed on a storage tank. The semi-porous cylindrical breakwater brought in not only a significant change in the wave field, but also a reasonable reduction in the hydrodynamic forces. Williams and Li [35] also evaluated the hydrodynamic forces on account of scattering of water waves by an array of surface-piercing bottom-mounted porous cylinders. Sankarbabu et al. [22] considered a similar type of structure and analyzed different impacts of wave and structure parameters on the array of cylinders. Recently, Sarkar and Bora [23–26] examined hydrodynamic force and wave run-up due to water wave interaction with different configurations of a specific type of compound porous cylinder and demonstrated through a number of numerical experiments that a change in the values of radius, draft, and porosity had a very significant influence on the hydrodynamic forces and wave run-up.

Lee and Chwang [11] solved the problems of scattering and radiation of water waves by thin vertical porous barriers in ocean of finite depth by converting the original boundary value problem to some dual series relations and then by applying the least square method. Li et al. [12] applied multi-term Galerkin method to investigate water wave interaction with vertical thin porous barriers. Das and Bora [7] discussed oblique water wave damping by two submerged thin vertical porous plates of different heights in finite ocean depth and observed that the porosity and location of the barriers affected the associated wave reflection. Manam and Sivanesan [19] came up with an analytical solution to the problem of scattering of deep water waves by a vertical porous barrier which was either fully submerged or surface-piercing. Sasmal et al. [27] considered the scattering of water waves by two unequal vertical porous barriers in infinite depth in which they took up both cases of the barriers being partially immersed and totally submerged. Recently, Chanda and Bora [3] considered water wave scattering by a breakwater in the form of two thin vertical submerged porous plates for a fluid flowing over a porous seabed and examined the effect of porosity of the seabed on the reflection characteristics.

The objective of all these works mentioned above was to understand the effect of a single porous structure on the wave flow. However, it has been established that a porous structure with a block-wise different porosity has a considerable

impact on the wave energy dissipation and trapping of oblique waves. Thus, at this point, it seems pertinent to provide a brief discussion on the works related to porous structures with multiple porosity to introduce a better picture to the mechanism of the problem considered in this work.

Mehaute [20] introduced a reasonable damping of wave energy due to a progressive wave absorber consisting of layers with different porosity and analyzed the effect of using multiple damping materials. He carried out experiments to analyze the effects of two-layer and three-layer porous structures, that is, for porous blocks with multiple porosities and friction factors. Sulisz [30] studied linear wave interaction with a composite breakwater in the form of a caisson on a multilayered rubble base to compute the associated wave reflection and transmission as well as the waveloads. It may be noted that the stability analysis for such a physical problem was carried out by him earlier (see Sulisz [29]). Twu et al. [31] studied the characteristics of oblique wave damping due to vertically placed porous breakwaters with different porosity in vertical strips. This study showed that the reflection coefficient of a multi-sliced structure decreased with an increasing angle of incidence. Lee and Cheng [10] considered a porous structure consisting of multiple regions with different values of porosity for wave reflection in which the domain resembled a combination of homogeneous rectangles. The formulation of the system used the flux and pressure conditions across vertical boundaries and interfaces, and then the problem was solved by using the orthogonal property of the depth dependent function of the corresponding wave motion within the porous layers. Liu and Faraci [14] analyzed wave reflection by a caisson, consisting of an open window on the front wall and an internal rubble mound (porous medium) with a slope, and the internal slope of the rubble mound that was assumed to be a series of horizontal porous steps. They obtained a semi-analytical solution to the problem by using eigenfunction expansions method. They also showed that the results matched reasonably well with the experimental data. Hu and Liu [8] developed a new floating multilayered breakwater for which a computer program AWAS-P was utilized for both oblique and normal incident waves. Lin et al. [13] studied the effect of a horizontal composite porous barrier in linear wave propagation. As an extension to their earlier problem in Hu and Liu [8], Hu et al. [9] derived an analytical solution for the problem of obliquely incident monochromatic wave scattering by a stationary rigid multilayered object having a rectangular cross section. Venkateswarlu and Karmakar [32] carried out a numerical investigation to study the reflection of water waves by multiple porous blocks of finite thickness with a finite spacing under the activity of oblique ocean waves by considering the leeward unbounded region and a confined region. The eigenfunction expansion method was used to analyze the effect of different porosities on the wave energy

dissipation. This observation showed that a better wave blocking could be accomplished by increasing the number of blocks with different porosity of the porous structures, and the confined region could be utilized for wave trapping. This seemed to be helpful in the design of porous structures. Venkateswarlu and Karmakar [33] further examined the hydrodynamic performance of a multilayered porous structure by evaluating the reflection coefficient corresponding to various depths, structure width and porosity. In this study, the step-like seabed was noticed to reduce the wave force on the leeward wall as compared to the uniform and elevated seabed in the presence of the layered porous block. In addition, the performance of the porous structure with multiple porous layers placed on the step-like seabed showed better results for the reflection coefficient as compared to the uniform and elevated seabed supported by the wall. Barman and Bora [1] considered the interaction of oblique surface gravity waves by a simple as well as a composite porous block of finite width placed on a multi-step bottom in a two-layer fluid. This study showed that, for a suitable configuration of the structure, an optimum width could be chosen for designing a breakwater of reasonable efficiency possessing both reflective and dissipative characteristics.

As per the authors’ best knowledge, study on reflection by porous structures, with various region-wise porosities, placed on a step-type bottom topography has never been considered earlier. The stratified porous structure on a step-type bottom topography is assumed to be more realistic and hence the expectation here is that the results will be more beneficial in designing appropriate breakwaters. Therefore, in the present study, we extend the work of Das and Bora [5] by dividing the porous structure under consideration into a number of vertical porous strips with each strip possessing a distinct porosity and placing it on a p -step bottom. The results are validated and compared with an existing one in the work of Das and Bora [5]. It is observed, as expected, that multiple porosities have a considerable impact on the reflection coefficient and hence on the wave energy dissipation as compared to the case of uniform porosity of the structure. It can be claimed that the present work is different from the rest of the earlier works (though the formulation has some similarity) in two aspects: consideration of p regions in the porous structure with each possessing a distinct porosity and an uneven seabed with a strip-wise depth which can be considered as an uneven bottom topography presenting a more realistic situation. The results presented here can be considered to be more general as compared to the earlier works, and it may be possible to derive some of the earlier results as particular cases. It is expected that this study has definite merit to get an optimized porous structure by the shuffling of porosity values in the blocks. Depending upon the location, the angle of incident-wave-attack on the near-shore structure changes. Therefore, the results of the above study can be utilized to get an efficient porous structure. This article is

arranged in the following manner: Sect. 2 consists of the mathematical formulation of the physical problem followed by the solution process in Sect. 3. The numerical results in graphical form along with the respective discussion of individual results are detailed in Sect. 4. The article ends in Sect. 5 with a brief conclusion highlighting the results along with the limitations and future scope of the current mathematical formulation.

2 Mathematical formulation

A wave motion of relatively small amplitude is considered within an undeformable porous structure in such a way that the porous structure possesses distinct porosity in each isotropic strip $x_i < x < x_{i+1}$ where the structure is placed on a p -step bottom and hence correspondingly it consists of p regions as shown in Fig. 1. A Cartesian coordinate system is chosen in such a way that the origin lies on the mean free surface $z = 0$ and the z -axis is positive in the upward direction. The uniform depth of the sea is h_1 prior to the steps and $h_i, 2 \leq i \leq p + 1$, corresponding to each step.

S_j in the j th region, which is different for different strips, has the following form:

$$S_j = 1 + C_M(1 - \gamma_j)/\gamma_j. \tag{1}$$

It is to be noted that $S_j = 1$ covers two distinct cases: $\gamma_j = 1$ implying no presence of structure; $C_M = 0$ implying the fluid under consideration to be inviscid. We denote the grain size of the porous material of the structure by d which is the main factor that affects the porosity. An iterative method corresponding to the porosity and the grain size of the porous material, as described by Madsen [17], is used to calculate the friction factor f . This procedure is detailed in “Appendix 1”.

The velocity potential for region I, i.e., in water region of depth $-h_1$, is given by

$$\begin{aligned} \Phi_w(x, y, z, t) &= \phi_w(x, z) \exp(i\lambda y - i\omega t); \\ -\infty < x < x_1, \quad -h_1 < z < 0, \end{aligned} \tag{2}$$

and the velocity potentials for all other regions, i.e., in porous regions at depth $-h_{j+1}$, are as follows:

$$\begin{aligned} \Phi_j(x, y, z, t) &= \phi_j(x, z) \exp(i\lambda y - i\omega t); \\ x_j < x < x_{j+1}, \quad -h_{j+1} < z < 0, \\ j &= 1, 2, \dots, p, \end{aligned} \tag{3}$$

where $x_1 = 0 < x_2 < x_3 < \dots < x_{p+1} = L$ with $x_{j+1} - x_j = l$ and $\lambda = k_{w,0} \sin \theta$.

Taking into account the governing equation and the associated boundary conditions, the boundary value problem (BVP) in region I can be written as

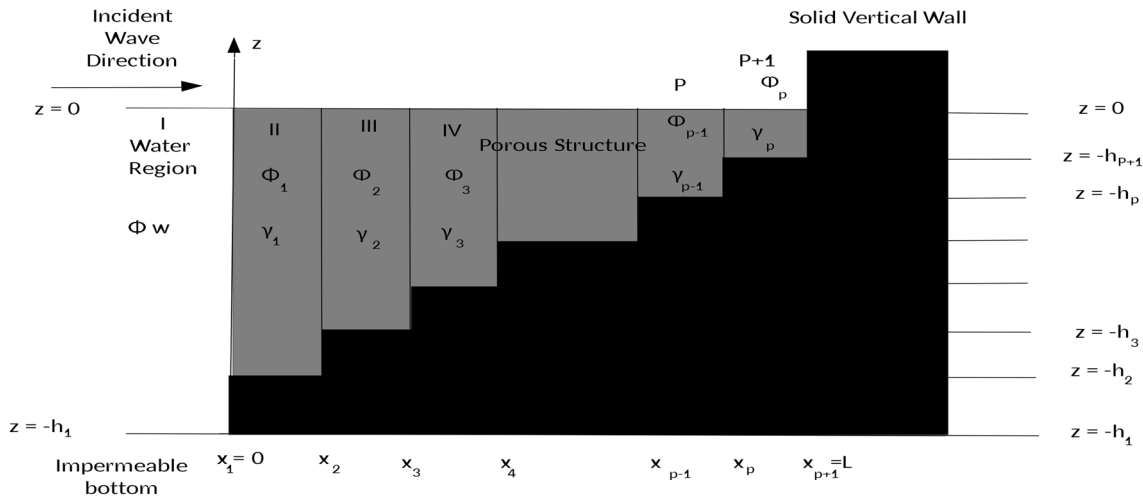


Fig. 1 Schematic diagram of wave propagation and the porous structure with a p -step bottom

$$\left(\frac{\partial^2}{\partial x^2} + \frac{\partial^2}{\partial z^2} - \lambda^2\right)\phi_w = 0; \quad -h_1 < z < 0, \quad -\infty < x < 0, \quad (4)$$

$$\frac{\partial \phi_w}{\partial z} - \Lambda \phi_w = 0; \quad z = 0, \quad -\infty < x < 0, \quad (5)$$

$$\frac{\partial \phi_w}{\partial z} = 0; \quad z = -h_1, \quad -\infty < x < 0, \quad (6)$$

$$\frac{\partial \phi_w}{\partial x} = 0; \quad x = 0, \quad -h_1 < z < -h_2, \quad (7)$$

where $\Lambda = \omega^2/g$. In a similar way, the BVP in the $(j + 1)$ th region ($j = 1, \dots, p$) consists of the following:

$$\left(\frac{\partial^2}{\partial x^2} + \frac{\partial^2}{\partial z^2} - \lambda^2\right)\phi_j = 0; \quad x_j < x < x_{j+1}, \quad -h_j < z < 0, \quad (8)$$

$$\frac{\partial \phi_j}{\partial z} - i\Lambda \tilde{R}_j \phi_j = 0; \quad x_j < x < x_{j+1}, \quad z = 0, \quad (9)$$

$$\frac{\partial \phi_j}{\partial z} = 0; \quad x_j < x < x_{j+1}, \quad z = -h_j, \quad (10)$$

$$\frac{\partial \phi_j}{\partial x} = 0; \quad x = x_{j+1}, \quad -h_{j+1} < z < -h_{j+2}, \quad j \neq p, \quad (11)$$

where $\tilde{R}_j = f_j - iS_j$ which has distinct values corresponding to distinct porous strips. When \tilde{R}_j and γ_j are constants for each j th porous strip, then the problem gets reduced to the one that was studied in Das and Bora [5].

The velocity potential ϕ_p satisfies Eqs. (8)–(10) along with the following extra condition:

$$\frac{\partial \phi_p}{\partial x} = 0; \quad x = x_{p+1} = L, \quad -h_{p+1} < z < 0. \quad (12)$$

In order to ensure the continuity of velocity and pressure across the vertical boundaries, the following conditions must be valid:

(i) Along $x = x_1 = 0, -h_2 \leq z \leq 0$:

$$\phi_w = i\tilde{R}_1 \phi_1, \quad (13)$$

$$\frac{\partial \phi_w}{\partial x} = \gamma_1 \frac{\partial \phi_1}{\partial x}. \quad (14)$$

(ii) Along $x = x_{j+1}, -h_{j+2} \leq z \leq 0, j = 1, 2, 3, \dots, p - 1$:

$$i\tilde{R}_j \phi_j = i\tilde{R}_{j+1} \phi_{j+1}, \quad (15)$$

$$\gamma_j \frac{\partial \phi_j}{\partial x} = \gamma_{j+1} \frac{\partial \phi_{j+1}}{\partial x}. \quad (16)$$

For complete understanding of the above four conditions, their derivation is detailed in “Appendix 2”.

3 Wave reflection by the multi-porosity structure

The velocity potential ϕ_w in the water region is evaluated as

$$\phi_w(x, z) = \{ \exp(iK_{w,0}x) + R_0 \exp(-iK_{w,0}x) \} Z_{1,0}(h_1, z) + \sum_{n=1}^N R_n \exp(-iK_{w,n}x) Z_{w,n}(h_1, z), \tag{17}$$

where $K_{w,n} = (k_{w,n}^2 - \lambda^2)^{1/2}$, with $k_{w,n}$ satisfying the following dispersion relation:

$$A = k_{w,n} \tanh(k_{w,n}h_1). \tag{18}$$

The associated depth-dependent function $Z_{w,n}(h_1, z)$ has the form

$$Z_{w,n}(h_1, z) = \frac{\cosh[k_{w,n}(h_1 + z)]}{\cosh(k_{w,n}h_1)}, \quad n = 0, 1, 2, \dots \tag{19}$$

Potentials $\phi_j(x, z)$ in the j th porous region, $j = 1, 2, 3, \dots, p$, are given by

$$\phi_j(x, z) = \begin{cases} \sum_{n=0}^N \{ A_{j,n} \exp[iK_{j,n}(x - x_j)] + B_{j,n} \exp[-iK_{j,n}(x - x_{j+1})] \} Z_{j,n}(h_{j+1}, z), & j = 1, 2, 3, \dots, p - 1, \\ \sum_{n=0}^N C_{p,n} \cos[K_{p+1,n}(x - L)] Z_{p,n}(h_{j+1}, z), & j = p, \end{cases} \tag{20}$$

where $A_{j,n}$, $B_{j,n}$ and $C_{p,n}$ are the coefficients to be determined and

$$K_{j,n} = (k_{j,n}^2 - \lambda^2)^{1/2}, \tag{21}$$

where $k_{j,n}$ satisfies the dispersion relation

$$i\tilde{R}_j A = k_{j,n} \tanh(k_{j,n}h_j), \quad j = 1, 2, 3, \dots, p, \quad \text{and} \tag{22}$$

for these regions, $Z_{j,n}(h_{j+1}, z)$ are the depth-dependent functions given by

$$Z_{j,n}(h_{j+1}, z) = \frac{\cosh[k_{j,n}(h_{j+1} + z)]}{\cosh(k_{j,n}h_{j+1})}, \quad j = 1, 2, 3, \dots, p. \tag{23}$$

The wave characteristics in the entire porous medium are represented by the complex wavenumbers $k_{m,n}$ where $m = w, 1, 2, 3, \dots$ and $n = 0, 1, 2, 3, \dots$. It is an established fact that the value of $k_{m,0}$ is purely real while those of $k_{m,n}$ ($n \geq 1$) are purely imaginary corresponding to a non-dissipative medium (i.e., $f = 0$). In the case of a dissipative medium, the friction factor f damps the wave motion through the addition of an imaginary part to $k_{m,0}$ and a real part to $k_{m,n}$, $n \geq 1$ (Das

and Bora [6]). Now using the matching conditions (13)–(14) and (15)–(16) along the boundaries $x = 0, -h_2 \leq z \leq 0$ and $x = x_{j+1}, -h_{j+2} \leq z \leq 0, j = 1, 2, \dots, p - 1$, we obtain

$$(1 + R_0)Z_{w,0} + \sum_{n=1}^N R_n Z_{w,n} = i\tilde{R}_1 \sum_{n=0}^N [A_{1,n} + B_{1,n} \exp(iK_{1,n}l)] Z_{1,n}, \tag{24}$$

$$K_{w,0}(1 - R_0)Z_{w,0} - \sum_{n=1}^N K_{w,n} R_n Z_{w,n} = \gamma_1 \sum_{n=0}^N [A_{1,n} - B_{1,n} \exp(iK_{1,n}l)] K_{1,n} Z_{1,n}, \tag{25}$$

$$\tilde{R}_j \sum_{n=0}^N [A_{j,n} \exp(iK_{j,n}l) + B_{j,n}] Z_{j,n} = \tilde{R}_{j+1} \sum_{n=0}^N [A_{j+1,n} + B_{j+1,n} \exp(iK_{j+1,n}l)] Z_{j+1,n}, \tag{26}$$

$$\gamma_j \sum_{n=0}^N [A_{j,n} \exp(iK_{j,n}l) - B_{j,n}] K_{j,n} Z_{j,n} = \gamma_{j+1} \sum_{n=0}^N [A_{j+1,n} - B_{j+1,n} \exp(iK_{j+1,n}l)] K_{j+1,n} Z_{j+1,n}. \tag{27}$$

Again, upon applying the matching conditions (15)–(16) along the boundary $x = x^p$, we obtain the following equations:

$$\tilde{R}_{p-1} \sum_{n=0}^N [A_{p-1,n} \exp(iK_{p-1,n}l) + B_{p-1,n}] Z_{p-1,n} = \tilde{R}_p \sum_{n=0}^N C_{p,n} Z_{p,n} \cos(K_{p,n}l), \tag{28}$$

$$i\gamma_{p-1} \sum_{n=0}^N [A_{p-1,n} \exp(iK_{p-1,n}l) - B_{p-1,n}] K_{p-1,n} Z_{p-1,n} = \gamma^p \sum_{n=0}^N C_{p,n} K_{p,n} Z_{p,n} \sin(K_{p,n}l). \tag{29}$$

Next, invoking the orthogonal property of $Z_{1,m}, Z_{j+1,m}, j = 1, 2, 3, \dots, p - 2$, and $Z_{p,m}, m = 0, 1, \dots, N$ in Eqs. (24)–(25), (26)–(27) and (28)–(29), respectively, the following equations are obtained:

$$\sum_{n=0}^N \beta_{w,n,m} R_n - i\tilde{R}_1 a_{1,m} A_{1,m} - i\tilde{R}_1 \exp(iK_{1,m}l) a_{1,m} B_{1,m} = -\beta_{w,0,m}, \tag{30}$$

$$\sum_{n=0}^N \beta_{w,n,m} k_{w,n} R_n + \gamma_1 K_{1,m} a_{1,m} A_{1,m} - \gamma_1 K_{1,m} \exp(iK_{1,m}l) a_{1,m} B_{1,m} = K_{w,0} \beta_{w,0,m}, \tag{31}$$

$$\tilde{R}_j \sum_{n=0}^N \exp(iK_{j,n}l) \beta_{j,n,m} A_{j,n} + \tilde{R}_j \sum_{n=0}^N \beta_{j,n,m} B_{j,n} - \tilde{R}_{j+1} a_{j+1,m} A_{j+1,m} - \tilde{R}_{j+1} \exp(iK_{j+1,n}l) a_{j+1,m} B_{j+1,m} = 0, \tag{32}$$

$$\gamma_j \sum_{n=0}^N K_{j,n} \exp(iK_{j,n}l) \beta_{j,n,m} A_{j,n} - \gamma_j \sum_{n=0}^N K_{j,n} \beta_{j,n,m} B_{j,n} - \gamma_j K_{j+1,m} a_{j+1,m} A_{j+1,m} - \gamma_{j+1} K_{j+1,m} \exp(iK_{j+1,n}l) a_{j+1,m} B_{j+1,m} = 0, \tag{33}$$

$$\tilde{R}_{p-1} \sum_{n=0}^N \exp(iK_{p-1,n}l) \beta_{p-1,n,m} A_{p-1,n} + \tilde{R}_{p-1} \sum_{n=0}^N \beta_{p-1,n,m} B_{p-1,n} - \tilde{R}_p a_{p,m} C_{p,m} \cos(K_{p,m}l) = 0, \tag{34}$$

$$i\gamma_{p-1} \sum_{n=0}^N K_{p-1,n} \exp(iK_{p-1,n}l) \beta_{p-1,n,m} A_{p-1,n} - i\gamma_{p-1} \sum_{n=0}^N K_{p-1,n} \beta_{p-1,n,m} B_{p-1,n} - \gamma_p K_{p,m} a_{p,m} C_{p,m} \sin(K_{p,m}l) = 0, \tag{35}$$

where

$$a_{q,m} = \int_{-h_q}^0 Z_{q,m}^2 dz = \frac{h_q \tanh(2K_{q,m}h_q)}{2K_{q,m}h_q \cosh(2K_{q,m}h_q)} \left(1 + \frac{2K_{q,m}h_q}{\sinh(2K_{q,m}h_q)} \right), \quad q = 1, 2, \dots, p, \tag{36}$$

$$\beta_{w,n,m} = \int_{-h_2}^0 Z_{w,n} Z_{1,m} dz = \frac{1}{K_{w,n}^2 - K_{1,m}^2} \left[\Lambda(1 - i\tilde{R}_1) - \frac{K_{w,n} \sinh[K_{w,n}(h_2 - h_1)]}{\cosh(K_{w,n}h_1) \cosh(K_{1,m}h_2)} \right], \tag{37}$$

$$\beta_{q,n,m} = \int_{-h_{q+2}}^0 Z_{q,n} Z_{q+1,m} dz = \frac{1}{K_{q,n}^2 - K_{q+1,m}^2} \left[-\frac{K_{q,n} \sinh[K_{q,n}(h_{q+2} - h_{q+1})]}{\cosh(K_{q,n}h_{q+1}) \cosh(K_{q+1,m}h_{q+2})} + i\Lambda(\tilde{R}_{q-1} - \tilde{R}_q) \right], \quad q = 1, 2, 3, \dots, p - 1. \tag{38}$$

Observe that Eq. (30) consists of $(N + 1)$, Eq. (31) of $(N + 1)$, Eq. (32) of $(p - 2) \times (N + 1)$, Eq. (33) of $(p - 2) \times (N + 1)$, Eq. (34) of $(N + 1)$, and Eq. (35) of $(N + 1)$ number of equations. Thus, we have a total of $(N + 1) + (N + 1) + (p - 2)(N + 1) + (p - 2)(N + 1) + (N + 1) + (N + 1) = 2p(N + 1)$ equations and there are $2p(N + 1)$ unknowns. Thus, Eqs. (30)–(35) reduce to the following system of linear algebraic equations:

$$AX = c \tag{39}$$

in which A is a square matrix of size $[2p(N + 1)]$ whose entries are evaluated by using Eqs. (36)–(38), the unknown vector is taken as $X = [R_0, \dots, R_N, A_{1,0}, B_{1,0}, \dots, A_{1,N}, B_{1,N}, \dots, A_{p-1,0}, B_{p-1,0}, \dots, A_{p-1,N}, B_{p-1,N}, C_{p,0}, \dots, C_{p,N}]^T$ and $c = [-\beta_{w,0,0}, \dots, -\beta_{w,0,N}, K_{w,0}\beta_{w,0,0}, \dots, K_{w,0}\beta_{w,0,N}, \underbrace{0, 0, \dots, 0}_{2(p-1)(N+1)\text{-times}}]^T$

whose value can be obtained from Eq. (37). Solving (39) and then evaluating R_0 will enable us to study the complete process of reflection within the porous structure along with the effect of various parameters.

4 Results and discussion

In this section, the computed results and the observations are thoroughly discussed. Here, the reflection coefficient is evaluated by solving the previously formulated system of Eq. (39) with the help of MATLAB R2020a version. For the computational purpose, the considered system is truncated after a particular value of N to determine the reflection coefficient by solving the truncated system of non-homogeneous linear equations. During this process, we first find the roots of the dispersion relations [Eqs. (18) and (22)], and the friction factor f for different porous regions. The roots $k_{w,n}$ and $k_{j,n}$ of the dispersion relations for different porous regions are found by the perturbation method utilized in Das and Bora [6]. The friction factor is numerically computed for some specific values of other parameters by using the secant method (see ‘‘Appendix 1’’ for details). Then the system of

equations is constructed by using all these preceding values. Finally, the reflection coefficient is evaluated by using the in-built inverse program.

Now, before discussing reflection phenomenon due to the specific porous structure under consideration, it is felt pertinent to validate one present result with an available one to confirm the effectiveness of the present mathematical model. In this context, we plot the reflection coefficient versus the dimensionless width of the porous structure in the present formulation and then compare it with the corresponding result (Fig. 21) of Das and Bora [5]. This is accomplished by considering the variation of $|R_0|$ against the angle of incidence θ for various values of h_{p+1}/h_1 with the number of steps = 8, $L/h_1 = 16$, $f = 1$, $N = 9$ and $\gamma = 0.9$. Figure 2 presents a very good validation of our result ensuring that the present model can be considered for further investigations.

In order to analyze the effect of various relevant parameters on the reflection coefficient, we consider the values of f and S as $f = 1, S = 1$. Further, the value of γ starts from 0.6 on the first porous strip ($x_1 < x < x_2$) and is distributed over the subsequent $(p - 1)$ strips in a monotonically increasing order while ending on the last strip with a value of 0.9. This shows that the structure has different porosity for different regions. This distribution of porosity values is fixed throughout the computation unless otherwise mentioned. In this way, the lee and shore-side faces of the structure have fixed values of porosity and, depending upon the number of steps, various multi-porosity values are constructed inside the structure. We name this

configuration as CONFIG-I(0.6, 0.9) for brevity. In other words, the porosity γ varies from 0.6 to 0.9 and since we take the number of steps to be 8, then the first strip would have porosity 0.6, the second strip would have porosity 6.0375, the third strip would have porosity 6.075, and so on. The values of porosity will be followed like-wise throughout. It may be mentioned here that for all the figures in this work, such porosity values are considered and this is not repeatedly mentioned in the figure captions and discussions.

Since we use $N = 9$ for all computation, now we justify why consideration of this value of N is sufficient. In Fig. 3, we plot the reflection coefficient $|R_0|$ against the incidence angle θ for different values of N ($N = 0, 2, 4, 6, 8, 10, 12$) along with the number of steps = 8, $h_{p+1}/h_1 = 0.5$, $L/h_1 = 2$.

This figure clearly justifies why the consideration of $N = 9$ is sufficient for all the observations to follow. Here, the reflection coefficient corresponding to $N = 2$, which is for two evanescent modes along with the propagating mode, changes significantly from the graph corresponding to the propagating mode ($N = 0$). It clearly shows the effect of the evanescent modes on the reflection coefficient. However, as we increase the number of evanescent modes, all the graphs almost coincide with each other from $N = 8$ onwards. Therefore, it is safe to assume that accurate results can be obtained by considering nine evanescent modes, which will also reduce the computational expense.

We also justify why the number of steps on the seabed is taken as 8 for our computation.

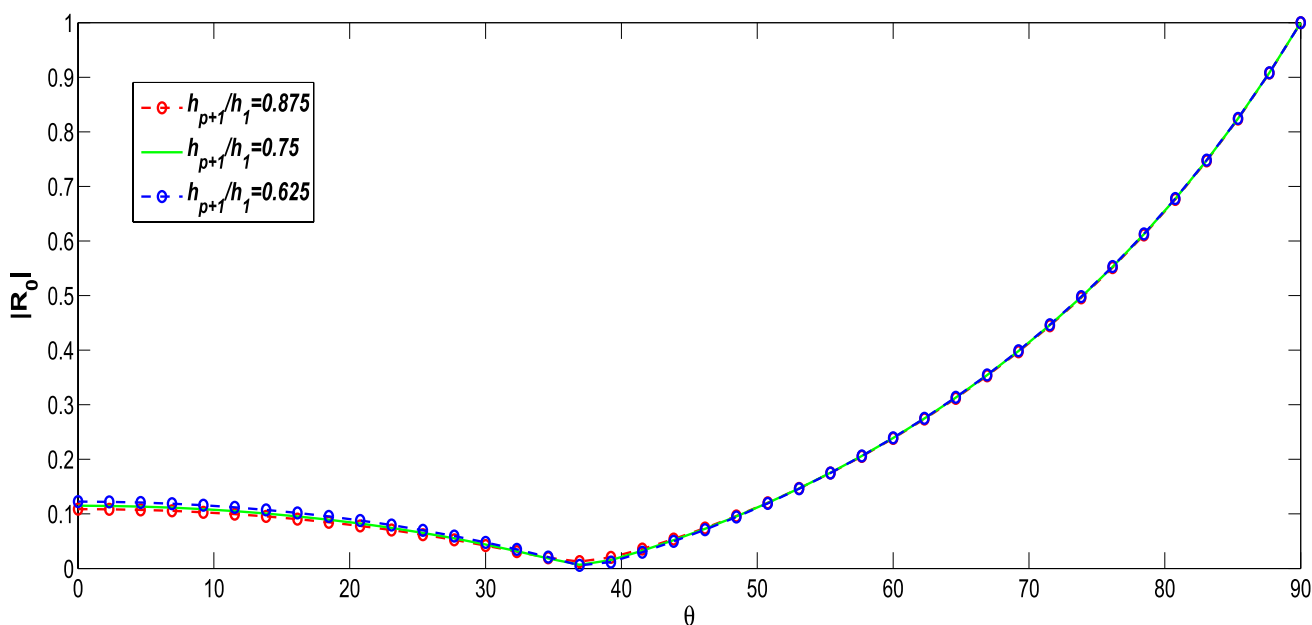


Fig. 2 Validation: reflection $|R_0|$ against incident wave angle θ for different depth h_{p+1}/h_1 with steps = 8, $L/h_1 = 16$, $f = 1$, $\gamma = 0.9$, $N = 9$ and $d/L = 0.0125$ where d is the grain size

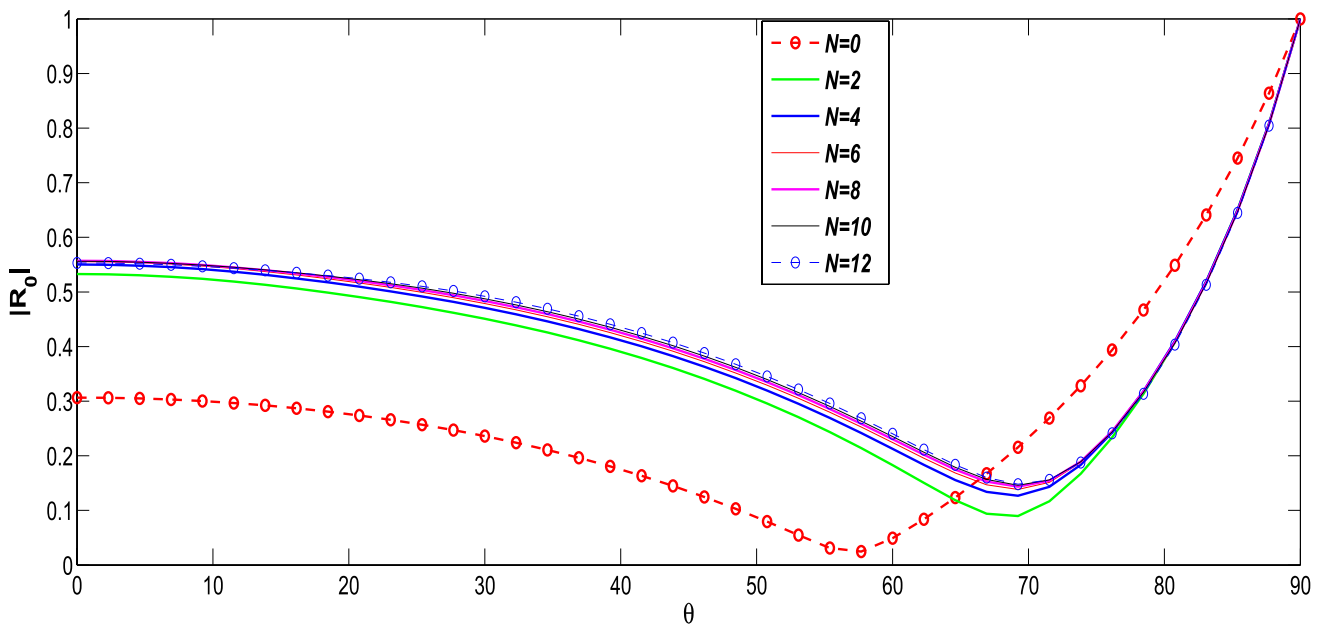


Fig. 3 $|R_0|$ against θ for different numbers of evanescent modes (N) with steps = 8, $h_{p+1}/h_1 = 0.5$, $f = 1$, $L/h_1 = 2$, $d/L = 0.0125$

Figure 4 corresponds to the reflection coefficient $|R_0|$ plotted against the angle of incidence θ corresponding to different number of steps: = 2, 4, 6, 8 and 10 along with $h_{p+1}/h_1 = 0.5$, $L/h_1 = 2$, $N = 9$. Here the angle of incidence has a wider range as compared to the case of the structure with uniform porosity.

This figure confirms why the consideration of 8 steps of the seabed is sufficient for all the observations. For the

number of steps as 2 and 4, the curves contrast with the curves for the number of steps more than 4. An increment in the number of steps gives a better convergence, but the variation in the reflection coefficient is negligible after 8 steps. Hence, for further investigation, we fix the number of steps as 8 to minimize the computational expenses.

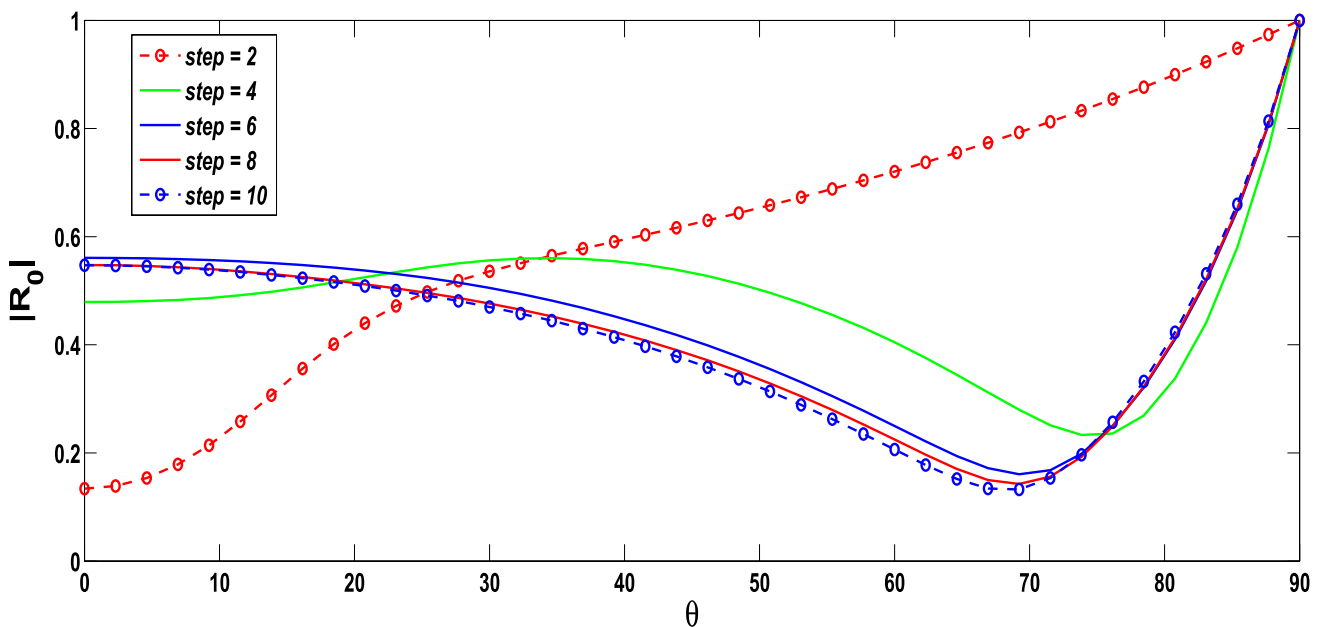


Fig. 4 Variation of $|R_0|$ against θ for different steps with $h_{p+1}/h_1 = 0.5$, $f = 1$, $L/h_1 = 2$, $N = 9$, $d/L = 0.0125$

Having validated our model from Fig. 2, we now plot the graph of $|R_0|$ against θ in Fig. 5 with the same data and having different porosity in each strip of the structure.

The magnitude of the reflection coefficient is noticed to increase as compared to the previous case for smaller values of θ . For each curve, a minimum of the reflection coefficient occurs corresponding to a higher value of θ . It is also observed that the reflection coefficient does not tend to 0 for any value of θ in contrast with the case of uniform porosity in Fig. 2. Here, the lowest porosity is toward the seaward direction, and the highest one is attached to the rigid wall. If the arrangement is reversed, it is expected that the reflection would be less. Although it is not tested, a different combination of porosity would result in different values of the reflection coefficient. Thus, it is possible to fine-tune the values of the reflection coefficient by changing the position of different vertical porous columns.

In Fig. 6, the reflection coefficient $|R_0|$ is plotted versus dimensionless width L/h_1 of the porous structure corresponding to four values of θ , namely, $0^\circ, 10^\circ, 20^\circ$ and 30° along with the number of steps = 8, $h_{p+1}/h_1 = 0.5$, $N = 9$. This figure shows that higher values of θ result in the reduction of values of the reflection coefficient. However, the reflection coefficient is observed to be independent of the value of θ after certain value of L/h_1 . It can further be observed that, for each value of θ , the curves take constant values after $L/h_1 = 1$. A similar pattern is observed for all other curves. Thus, the variation in the reflection coefficient occurs till the width L/h_1 of the porous structure becomes less than 1.

Figure 7 examines the effect of angle of incidence θ on the reflection coefficient $|R_0|$ corresponding to various values of h_{p+1}/h_1 , namely 1.5, 2, 2.5 and 3 along with $L/h_1 = 2$, $N = 9$. The observation is that, with an increase in the value of h_{p+1}/h_1 , the value of the reflection coefficient decreases approximately up to $\theta = 69^\circ$ and the process gets reversed after this value before converging to 1 at $\theta = 90^\circ$. This convergence of the graphs is due to the passing of waves tangentially to the seaward surface, without penetrating the porous structure. The existence of a minimum value of the reflection coefficient suggests the existence of a critical angle for maximum effectiveness of the porous structure. This helps in positioning the breakwater in a specific location where the direction of wave attack is known.

Figure 8 shows the behavior of $|R_0|$ against θ for different values of $\Lambda h_1 = 0.5, 1, 2$ along with $h_{p+1}/h_1 = 0.5$, $L/h_1 = 2$, $N = 9$. It shows that the magnitude of the reflection coefficient reduces with an increase in the wavenumber. It is observed that, for short waves (higher wavenumber), the reflection coefficient decreases up to $\theta \approx 63^\circ$ and the same goes for long waves whereas the reflection coefficient is higher for relatively long waves for a porous structure with uniform porosity which makes the problem and solution more realistic. This figure exhibits exactly the same behavior as in Fig. 7 which also matches significantly the pattern where the monotonicity of the graph gets changed. For relatively short waves (large Λh_1), the angle of incidence at which the minimum reflection occurs takes smaller values as compared to the long waves.

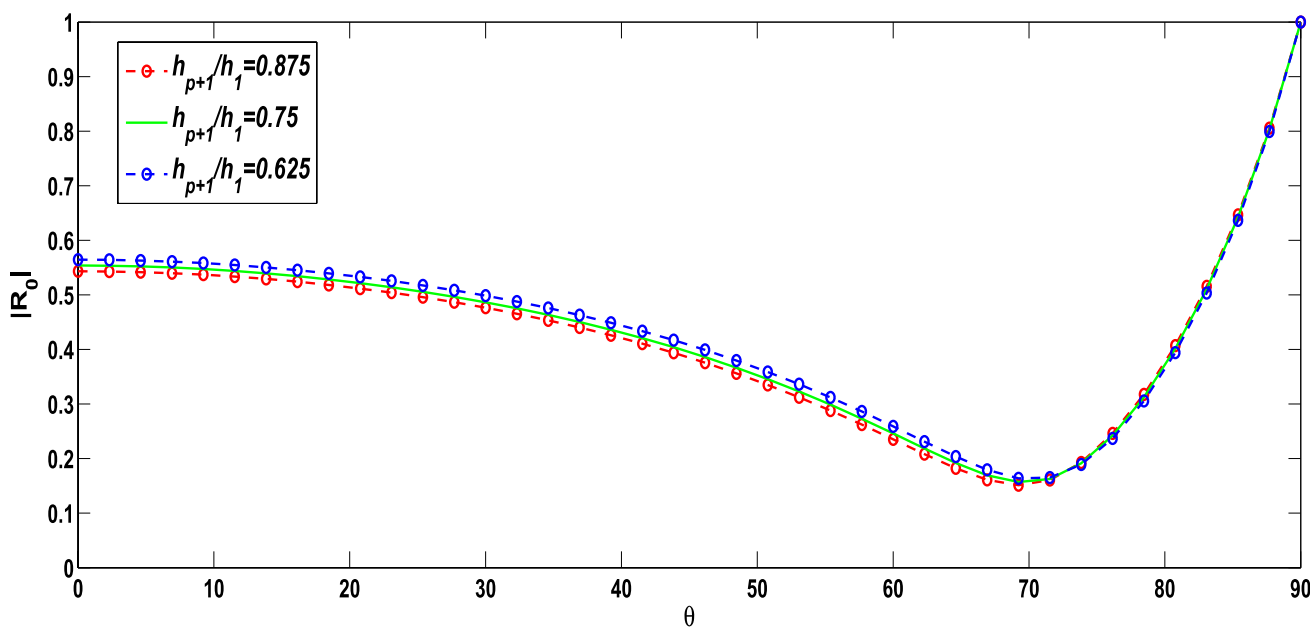


Fig. 5 Variation of $|R_0|$ against incident wave angle (θ) for different h_{p+1}/h_1 with steps = 8, $L/h_1 = 16$, $f = 1$, $N = 9$, $d/L = 0.0125$

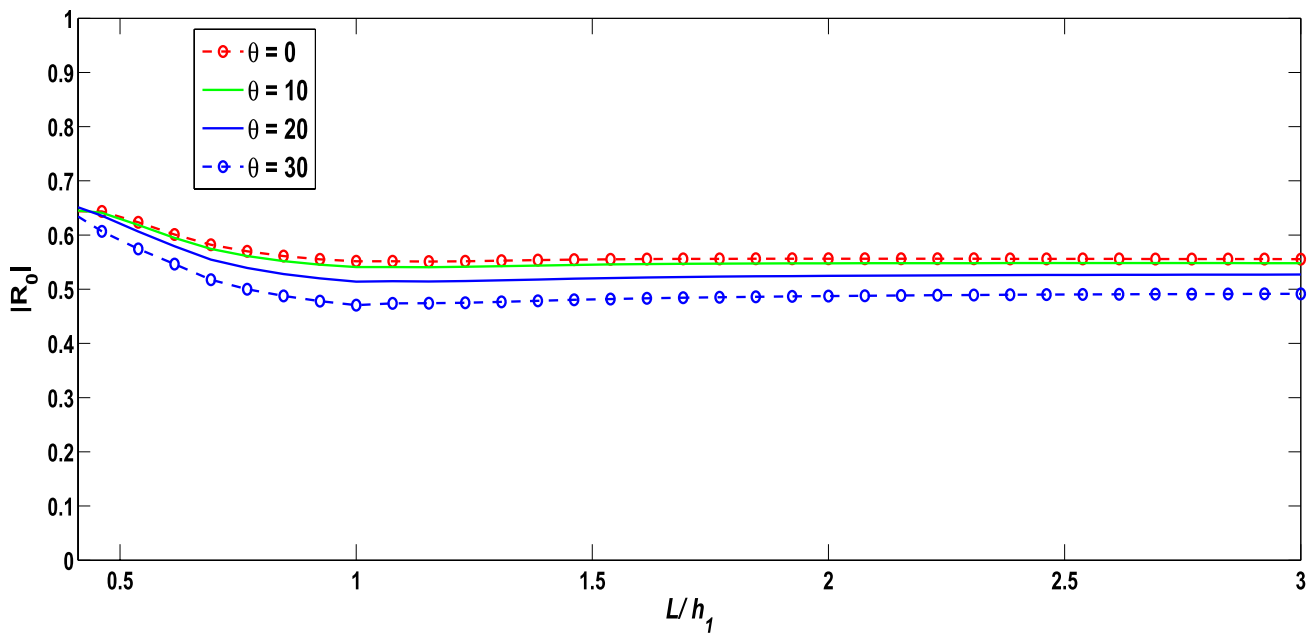


Fig. 6 Reflection coefficient $|R_0|$ against dimensionless width of the porous structure (L/h_1) for different θ with steps = 8, $h_{p+1}/h_1 = 0.5$, $f = 1$, $N = 9$, $d/L = 0.0125$

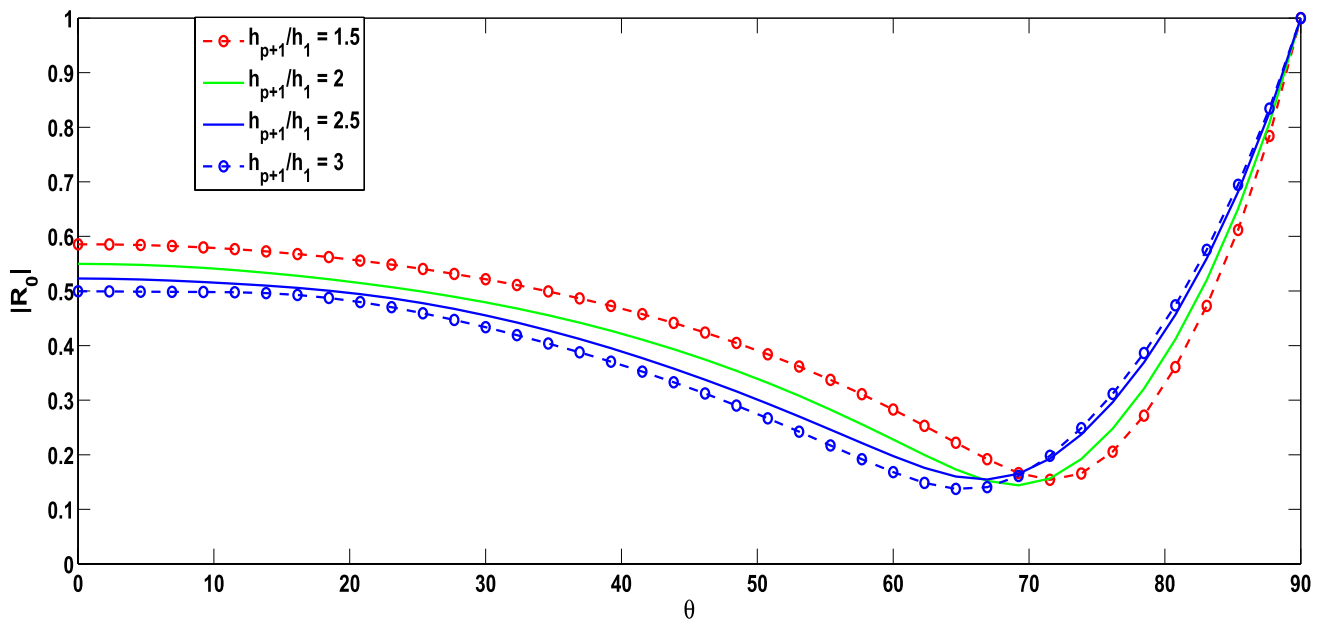


Fig. 7 Variation of $|R_0|$ against θ for different h_{p+1}/h_1 with $f = 1$, $L/h_1 = 2$, $N = 9$, $d/L = 0.0125$

Figure 9 presents $|R_0|$ against θ corresponding to various values of d/L such as 0.00625, 0.009375, 0.0125, 0.015625, 0.01875, 0.025, 0.03125 and 0.0375 along with $h_{p+1}/h_1 = 0.5$, $L/h_1 = 2$, $N = 9$. Corresponding to an increase in the value of d/L , a reduction in the value of the reflection coefficient takes place. Consequently, a significant change in the minimum of the reflection coefficient and its occurrence-angle are observed. For

example, the minimum reflection coefficient is below 0.1 for $d/L = 0.0375$ and occurs at $\theta \approx 63^\circ$, whereas the same is around 0.2 occurring at $\theta \approx 74^\circ$ for the same value of d/L . This observation can be utilized as the working principle for choosing the grain size in controlling the reflection coefficient once the incident wave direction is known at any particular location. It will also optimize the cost of preparing the porous material.

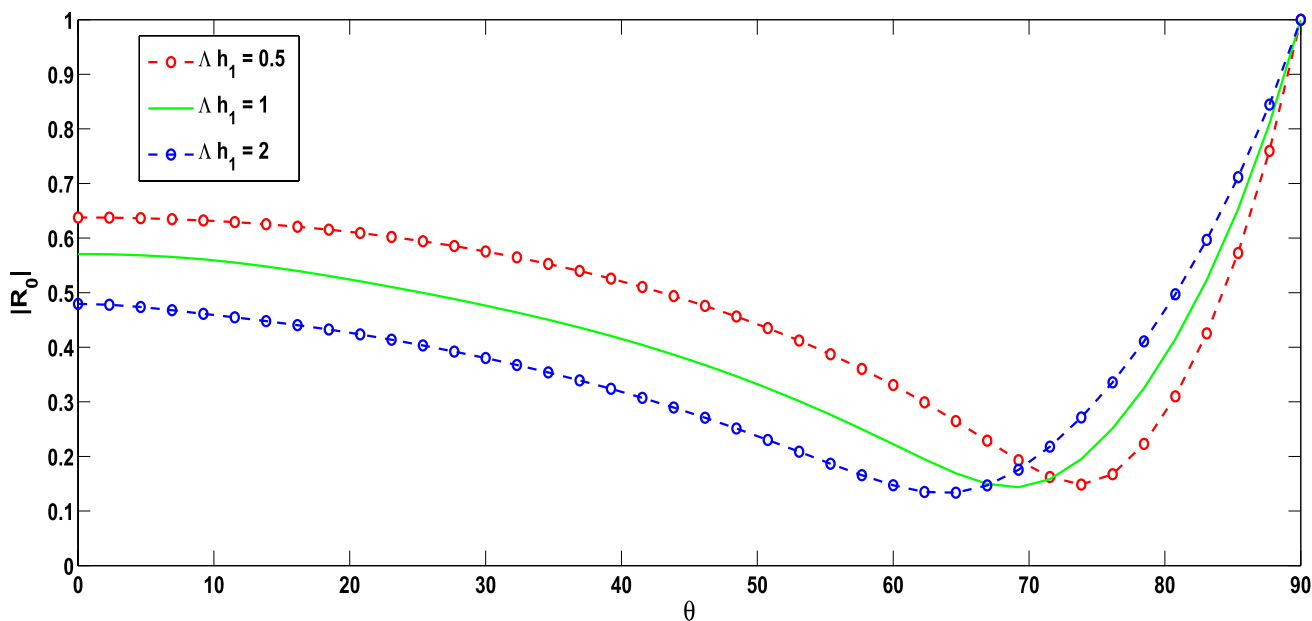


Fig. 8 Variation of $|R_0|$ against θ for different λh_1 with $h_{p+1}/h_1 = 0.5$, $f = 1$, $L/h_1 = 2$, $N = 9$, $d/L = 0.0125$

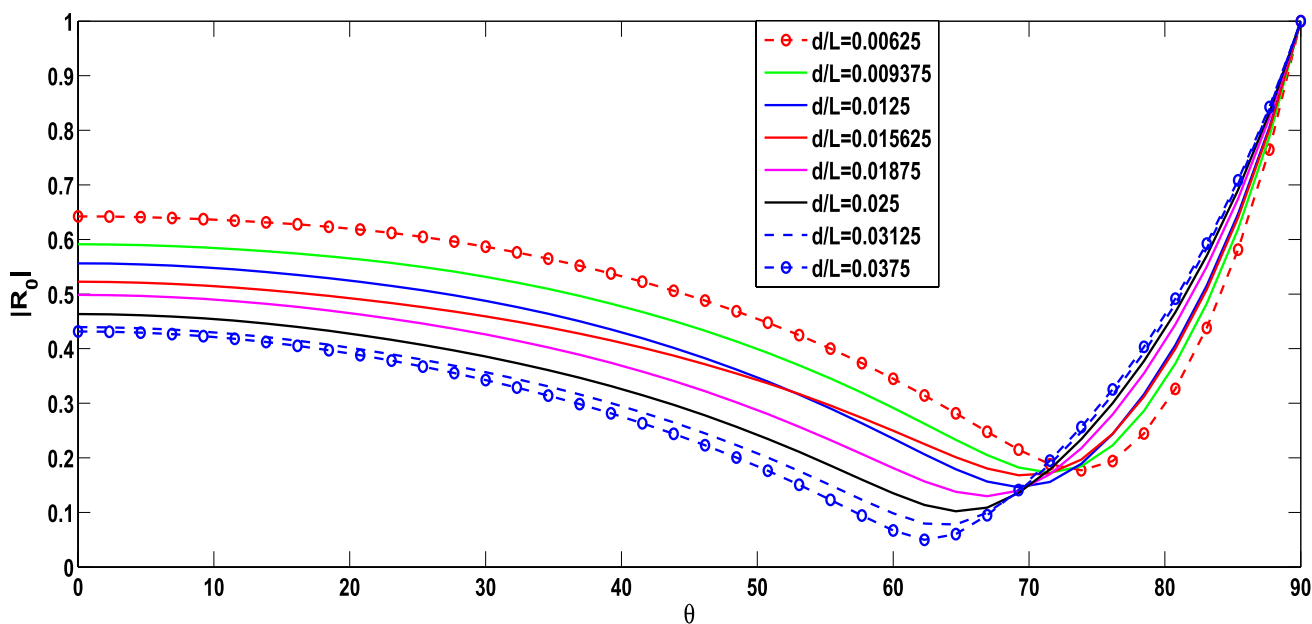


Fig. 9 Variation of $|R_0|$ against θ for different d/L with $h_{p+1}/h_1 = 0.5$, $f = 1$, $L/h_1 = 2$, $N = 9$, $d/L = 0.0125$

5 Conclusion

This article studies the wave reflection and damping by a vertical porous structure, with different strip-wise porosities, placed on a step-like seabed. By defining velocity potentials in a number of sub-domains and utilizing the available boundary and matching conditions, a system of linear equations is derived with the help of linear wave

theory and eigenfunction expansion method. The validity of the proposed model is performed by matching it with an existing result. For this specific formulation, when the seaward face of the structure is less porous, a higher reflection coefficient is observed in comparison with a uniform porous structure. But fine-tuning of the reflection coefficient is possible by shuffling the position of the individual porous columns. There also exists an optimum width of the porous structure beyond which the reflection

coefficient stabilizes. The existence of such a width will help to minimize the construction cost of the breakwater. It is observed that, up to a critical value, lower values of the reflection coefficient correspond to comparatively higher values of the angle of incidence. Thus, the multi-porosity porous structure gives a wider range of the angles of incidence for which the reflection coefficient keeps decreasing as compared to the uniform porosity and it can be considered more advantageous to position the breakwater relative to the incoming wave direction. It is also observed that, for short waves, the reflection coefficient decreases and the same happens also for long waves whereas the reflection coefficient is higher for relatively long waves when uniform porosity is considered. Subsequently, this makes the model with a multi-porosity structure a more suitable one from the practical point of view. Although not discussed in the present work, it will be possible to approximate any arbitrary ocean bottom topography with a non-homogeneous/multi-porous structure placed atop by following the present method. By changing the number of steps and their respective width and height, a desired bottom configuration can be achieved. Due to the complexity, such a physical problem is not attempted here, but definitely there is a promising scope in future to tackle it. Further, an optimized porous structure can be engineered with the help of the porosity shuffling as mentioned earlier. In that case, an efficient mathematical model can be implemented to validate a complicated breakwater system to protect shorelines, harbors, ports from high wave attack. Use of multiple porosities in the breakwater structure adds more efficiency to the wave blocking. In other words, use of a stratified porous structure has immense contribution in protecting various shoreline and offshore facilities by attenuating the wave height. In a nutshell, by considering a step-like seabed and putting vertical columns of different porous material over each step, a non-homogeneous porous breakwater on arbitrary undulating seabed can be mathematically approximated. Although not taken up now due to its higher degree of complexity, this work provides the stepping stone for such type of mathematical approximation to a fairly complex physical problem.

Appendices

Appendix 1: Computation of friction factor (f)

The friction factor (f) depends on the incoming wave amplitude (a_i) as well as on the characteristics of the porous structure. We follow the procedure by Madsen [17] for the evaluation of the friction factor corresponding to the porosity γ . By employing the secant method, we numerically solve for f

with two initial choices of friction factor as $f = 0$ and $f = 1$. We have

$$G \equiv \alpha_0 \frac{(1-\gamma)^3}{\gamma} \left(\frac{\nu T}{2\pi d^2} \right) + \beta_0 \frac{(1-\gamma)}{\gamma^2} \frac{a_i}{2\pi d} T \sqrt{\frac{g}{h_2}} \Lambda - f = 0,$$

where $\alpha_0 = 1000$, $\beta_0 = 2.8$, ν denotes kinematic viscosity, T denotes wave period, d the grain size of the porous material, a_i the incident wave amplitude and

$$\Lambda = \frac{\int_0^L \int_0^T |U^*| U^{*2} dt dx}{\int_0^L U^{*2} dt dx},$$

$$U^* = Re \left\{ \frac{2\varepsilon [\exp(-ikx) - \exp\{ik(x-2L)\}]}{1 + \varepsilon + (1 - \varepsilon) \exp(-i2kL)} \exp(i\omega t) \right\},$$

with $\varepsilon = \gamma / \sqrt{1 - if}$ and $k = \omega \sqrt{1 - if} / \sqrt{gh_2}$.

Appendix 2: Derivation of continuity conditions

Let us consider U_w and U_j , respectively, to be the velocities of a fluid at any point inside the water and the j th porous region attached to each other. Then the following relation holds true:

$$U_j = \nabla \Phi_j \quad j = 1, 2, 3, \dots, p, \quad \text{in the water region.} \quad (40)$$

Now, inside the porous region

$$\begin{aligned} S_j \frac{\partial U_j}{\partial t} &= -\frac{\nabla P_j}{\rho} - f_j \omega U_j \\ \implies S_j \frac{\partial \Phi_j}{\partial t} &= -\frac{P_j}{\rho} - f_j \omega \Phi_j \\ \implies -i\omega S_j \phi_j &= -\frac{P_j}{\rho} - f_j \omega \phi_j \\ \implies \omega(f_j - iS_j)\phi_j &= -\frac{P_j}{\rho} \\ \implies \omega \tilde{R}_j \phi_j &= -\frac{P_j}{\rho}, \end{aligned} \quad (41)$$

where P_w and P_j are the dynamic pressures of the water and porous regions, respectively.

In the water region, Bernoulli's equation gives

$$\begin{aligned} \frac{\partial U_w}{\partial t} &= -\frac{\nabla P_w}{\rho} \\ \implies \frac{\partial \Phi_w}{\partial t} &= -\frac{P_w}{\rho} \\ \implies -i\omega \phi_w &= -\frac{P_w}{\rho}. \end{aligned} \quad (42)$$

Now, along the vertical boundary between the water and porous regions, continuity of pressure ($P_w = P_j$) results in [from Eqs. (41) and (42)] the following matching condition:

$$\phi_w = i\tilde{R}_j\phi_j. \quad (43)$$

Mass flux per unit volume and unit time inside the porous region is $\rho\mathbf{U}\gamma$ and the same inside the water region is $\rho\mathbf{U}$. Along the vertical boundary, the continuity of mass flux implies

$$\begin{aligned} \rho\mathbf{U}_w &= \rho\mathbf{U}_j\gamma_j, \\ \implies \frac{\partial\phi_w}{\partial x} &= \gamma_j \frac{\partial\phi_j}{\partial x} \end{aligned} \quad (44)$$

along the x -direction.

Acknowledgements The first author wishes to thank Department of Mathematics, Indian Institute of Technology Guwahati, India where this work was initiated during her M.Sc. All the authors express their gratitude to the two esteemed reviewers for their comments and suggestions catering to which a much improved revised version has resulted, and also to the Editor-in-Chief Professor Toru Sato for giving an opportunity to revise the manuscript.

References

1. K.K. Barman, S.N. Bora, Linear water wave interaction with a composite porous structure in a two-layer fluid flowing over a step-like sea-bed. *Geophys. Astrophys. Fluid Dyn.* (2020). <https://doi.org/10.1080/03091929.2020.1842391>
2. P.G. Chamberlain, D. Porter, The modified mild-slope equation. *J. Fluid Mech.* **291**, 393–407 (1995). <https://doi.org/10.1017/S0022112095002758>
3. A. Chanda, S.N. Bora, Effect of a porous sea-bed on water wave scattering by two thin vertical submerged porous plates. *Eur. J. Mech. B* **84**, 250–261 (2020). <https://doi.org/10.1016/j.euromechflu.2020.06.009>
4. S. Das, S.N. Bora, Damping of oblique ocean waves by a vertical porous structure placed on a multi-step bottom. *J. Mar. Sci. Appl.* **13**(4), 362–376 (2014). <https://doi.org/10.1007/s11804-014-1281-7>
5. S. Das, S.N. Bora, Reflection of oblique ocean water waves by a vertical porous structure placed on a multi-step impermeable bottom. *Appl. Ocean Res.* **47**, 373–385 (2014). <https://doi.org/10.1016/j.apor.2014.07.001>
6. S. Das, S.N. Bora, Reflection of oblique ocean water waves by a vertical rectangular porous structure placed on an elevated horizontal bottom. *Ocean Eng.* **82**, 135–143 (2014). <https://doi.org/10.1016/j.oceaneng.2014.02.035>
7. S. Das, S.N. Bora, Oblique water wave damping by two submerged thin vertical porous plates of different heights. *Comput. Appl. Math.* **37**, 3759–3779 (2018). <https://doi.org/10.1007/s40314-017-0545-7>
8. J. Hu, P.L.F. Liu, A unified coupled-mode method for wave scattering by rectangular-shaped objects. *Appl. Ocean Res.* **79**, 88–100 (2018). <https://doi.org/10.1016/j.apor.2018.07.008>
9. J. Hu, Y. Zhao, P.L.F. Liu, A model for obliquely incident wave interacting with a multi-layered object. *Appl. Ocean Res.* **87**, 211–222 (2019). <https://doi.org/10.1016/j.apor.2019.03.004>
10. J.F. Lee, Y.M. Cheng, A theory for waves interacting with porous structures with multiple regions. *Ocean Eng.* **34**(11–12), 1690–1700 (2007). <https://doi.org/10.1016/j.oceaneng.2006.10.012>
11. M.M. Lee, A.T. Chwang, Scattering and radiation of water waves by permeable barriers. *Phys. Fluids* **12**, 54–65 (2000). <https://doi.org/10.1063/1.870284>
12. A.J. Li, Y. Liu, H.J. Li, Accurate solutions to water wave scattering by vertical thin porous barriers. *Math. Probl. Eng.* **2015**, 11 (2015). <https://doi.org/10.1155/2015/985731>
13. Q. Lin, Q.R. Meng, D.Q. Lu, Waves propagating over a two-layer porous barrier on a sea-bed. *J. Eng. Math.* **30**, 453–462 (2019). <https://doi.org/10.1007/s42241-018-0041-6>
14. Y. Liu, C. Faraci, Analysis of orthogonal wave reflection by a caisson with open front chamber filled with sloping rubble mound. *Coast. Eng.* **91**, 151–163 (2014). <https://doi.org/10.1016/j.coastaleng.2014.05.002>
15. I.J. Losada, R.A. Dalrymple, M.A. Losada, Water waves on crown breakwaters. *J. Waterw. Port Coast. Ocean Eng.* **119**(4), 367–380 (1993). [https://doi.org/10.1061/\(ASCE\)0733-950X\(1993\)119:4\(367\)](https://doi.org/10.1061/(ASCE)0733-950X(1993)119:4(367))
16. O.S. Madsen, Wave transmission through porous structures. *J. Waterw. Div. ASCE* **100**(3), 169–188 (1974). <https://doi.org/10.1061/AWHCAR.0000242>
17. P.A. Madsen, Wave reflection from a vertical permeable wave absorber. *Coast. Eng.* **7**(4), 381–396 (1983). [https://doi.org/10.1016/0378-3839\(83\)90005-4](https://doi.org/10.1016/0378-3839(83)90005-4)
18. V. Mallayachari, V. Sundar, Reflection characteristics of permeable seawalls. *Coast. Eng.* **23**(1–2), 135–150 (1994). [https://doi.org/10.1016/0378-3839\(94\)90019-1](https://doi.org/10.1016/0378-3839(94)90019-1)
19. S.R. Manam, M. Sivanesan, Scattering of water waves by vertical porous barriers: an analytical approach. *Wave Motion* **67**, 89–101 (2016). <https://doi.org/10.1016/j.wavemoti.2016.07.008>
20. L. Mehaute, Progressive wave absorber. *J. Hydraul. Res.* **10**, 153–169 (1972). <https://doi.org/10.1080/00221687209500026>
21. D. Porter, D.J. Staziker, Extensions of the mild-slope equation. *J. Fluid Mech.* **300**, 367–382 (1995). <https://doi.org/10.1017/S0022112095003727>
22. K. Sankarbabu, S.A. Sannasiraj, V. Sundar, Interaction of regular waves with a group of dual porous circular cylinders. *Appl. Ocean Res.* **29**, 180–190 (2007). <https://doi.org/10.1016/j.apor.2008.01.004>
23. A. Sarkar, S.N. Bora, Hydrodynamic forces due to water wave interaction with a bottom-mounted surface-piercing compound porous cylinder. *Ocean Eng.* **171**, 59–70 (2019). <https://doi.org/10.1016/j.oceaneng.2018.10.019>
24. A. Sarkar, S.N. Bora, Water wave diffraction by a surface-piercing floating compound porous cylinder in finite depth. *Geophys. Astrophys. Fluid Dyn.* **113**, 348–376 (2019). <https://doi.org/10.1080/03091929.2019.1626377>
25. A. Sarkar, S.N. Bora, Hydrodynamic coefficients for a floating semi-porous compound cylinder in finite ocean depth. *Mar. Syst. Ocean Technol.* **15**, 270–285 (2020). <https://doi.org/10.1007/s40868-020-00086-0>
26. A. Sarkar, S.N. Bora, Hydrodynamic forces and moments due to interaction of linear water waves with truncated partial-porous cylinders in finite depth. *J. Fluid. Struct.* **94**, 102898 (2020). <https://doi.org/10.1016/j.jfluidstructs.2020.102898>
27. A. Sasmal, S. Paul, S. De, Effect of porosity on oblique wave diffraction by two unequal vertical porous barriers. *J. Mar. Sci. Appl.* **18**, 417–432 (2019). <https://doi.org/10.1007/s11804-019-00107-4>
28. C.K. Sollitt, R.H. Cross, Wave transmission through permeable breakwaters. In: *Proceedings of the 13th Coastal Engineering Conference, Vancouver (ASCE, Virginia, 1973)*, pp. 1827–1846. <https://doi.org/10.9753/icce.v13.99>
29. W. Sulisz, Stability analysis for multilayered rubble bases. *J. Waterw. Port Coast. Ocean Eng.* **120**(3), 269–282 (1994). [https://doi.org/10.1061/\(ASCE\)0733-950X\(1994\)120:3\(269\)](https://doi.org/10.1061/(ASCE)0733-950X(1994)120:3(269))

30. W. Sulisz, Wave loads on caisson founded on multilayered rubble base. *J. Waterw. Port Coast.* **123**(3), 91–101 (1997). [https://doi.org/10.1061/\(ASCE\)0733-950X\(1997\)123:3\(91\)](https://doi.org/10.1061/(ASCE)0733-950X(1997)123:3(91))
31. S.W. Twu, C.C. Liu, C.W. Twu, Wave damping characteristics of vertically stratified porous structures under oblique wave action. *Ocean Eng.* **29**(11), 1295–1311 (2002). [https://doi.org/10.1016/S0029-8018\(01\)00091-9](https://doi.org/10.1016/S0029-8018(01)00091-9)
32. V. Venkateswarlu, D. Karmakar, Numerical investigation on the wave dissipating performance due to multiple porous structures. *ISH J. Hydraul. Eng.* (2019). <https://doi.org/10.1080/09715010.2019.1615393>
33. V. Venkateswarlu, D. Karmakar, Significance of sea-bed characteristics on wave transformation in the presence of stratified porous block. *Coast. Eng. J.* **62**, 1–22 (2020). <https://doi.org/10.1080/21664250.2019.1676366>
34. A.N. Williams, W. Li, Wave interaction with a semi-porous cylindrical breakwater mounted on a storage tank. *Ocean Eng.* **25**, 195–219 (1998). [https://doi.org/10.1016/S0029-8018\(97\)00006-1](https://doi.org/10.1016/S0029-8018(97)00006-1)
35. A.N. Williams, W. Li, Water wave interaction with an array of bottom-mounted surface-piercing porous cylinders. *Ocean Eng.* **27**, 841–866 (2000). [https://doi.org/10.1016/S0029-8018\(99\)00004-9](https://doi.org/10.1016/S0029-8018(99)00004-9)
36. X. Yu, Diffraction of water waves by porous breakwaters. *J. Waterw. Port Coast. Ocean Eng.* **121**, 275–282 (1995). [https://doi.org/10.1061/\(ASCE\)0733-950X\(1995\)121:6\(275\)](https://doi.org/10.1061/(ASCE)0733-950X(1995)121:6(275))
37. S. Zhu, Water waves within a porous medium on an undulating bed. *Coast. Eng.* **42**(1), 87–101 (2001). [https://doi.org/10.1016/S0378-3839\(00\)00050-8](https://doi.org/10.1016/S0378-3839(00)00050-8)

Publisher's Note Springer Nature remains neutral with regard to jurisdictional claims in published maps and institutional affiliations.